ENVIRONMENTAL SCIENCES 2001 Vol. 10, No. S-1, 11~22
Bulletin of the Korean Environmental Sciences Society

Parameterization of Along-Wind Dispersion Coefficients based on Field and Wind Tunnel Data

Sung-Dae Kang

Meteorological Research Institute Korea Meteorological Administration Seoul 156-720, Korea

(Manuscript received on December 19, 2000)

Observations related to the along-wind dispersion of puffs were collected from 13 field sites and from a wind tunnel experiment and used to test simple similarity relations. Because most of the data made use of concentration time series observations from fixed monitors, the basic observation was t, the standard deviation of the concentration time series. This data also allowed the travel time, t, from the source to the receptor to be estimated, from which the puff advective speed, ue, could be determined. The along-wind dispersion coefficient, x, was then assumed to equal tue. The data, which extended over four orders of magnitude, supported the similarity relations t = 0.1 t and x = 1.8 u* t, where t is the travel time and u* is the friction velocity. About 50 % of the observations were within a factor of two of the predictions based on the similarity relations.

Key words : air pollution, dispersion coefficient, puff model

1. Introduction

Models for the transport and dispersion of puffs must be able to parameterize the along-wind dispersion coefficient, x, and the effective speed, ue, at which the puff is moving. In the case of puffs released near the ground, the effective speed, ue, increases as the puff moves downwind, since the puff's vertical size continually increases. While there are already several similarity-based theoretical models of along-wind dispersion available[1~3], there are very few field data sets that can be used for model development and evaluation.

Fortunately there have been several high-quality puff-dispersion experiments carried out during the past few years, and the data has recently become available. In each of these experiments, the puff release was in a layer within 100 m from the ground, for example, at the Dugway Proving Ground and at two separate locations at the Nevada Test Site (Yucca Flat and Frenchman Flat). The new data have been combined with several sets of older data, including releases near the ground and at elevations of about 100 m, in order to determine if the data follow some simple similarity relations. Accordingly, this paper describes the theoretical background for along-wind dispersion, reviews the experiments, presents some tables and figures of the key observations, and suggests some simplified formulas for the along-wind dispersion coefficient, x.

2. Theoretical Considerations and Methods of Analysis

a. Basic Similarity Formulas and Assumptions

Gaussian models of puff dispersion make use of the along-wind dispersion coefficient, x[4]. As has been established for almost 50 years, dispersion is influenced by the mean wind shear as well as turbulence[5]. Early theoretical analyses were concerned with both the along-wind component of dispersion, x, and the cross-wind component of dispersion, y. Since the boundary layer nearly always contains a cross-wind direction shear(averaging about 30 degrees), due to the balance of pressure, Coriolis, and drag forces, the contribution of shear to cross-wind dispersion, y, becomes significant for puffs, which have been transported for mesoscale distances, when the

puff's vertical size is a significant fraction of the boundary layer depth.

Near the ground, the along-wind speed shear is much larger than the cross-wind direction shear, and therefore puffs have been observed to be elongated in the x direction(more cigar-shaped than spherical). Simple theoretical formulas for calculating the effects of along-wind or cross-wind shears on x or y, respectively, have been developed by Pasquill[6] and Csanady[7]. The Chatwin[1] and Wilson[3] approaches represent the same type of derivation, and all of these authors followed Saffmans[8] and Smiths[9] theoretical analysis. In the latter, the following formula is suggested:

$$x2 = xt2 + xs2 \quad (1)$$

where the first term represents the contribution due to ambient turbulence and the second term represents the contribution due to wind shear. These terms can be expressed as follows:

$$xt = A\ u^*\ t \quad (2)$$

$$xs = B\ (1/121/2)\ z\ (du/dz)\ t \quad (3)$$

where u* is the friction velocity, t is the travel time, u is the mean wind speed, z the height , and A and B are constants that can initially be assumed to equal about one and then be calibrated with data. The factor of 1/121/2 is the conversion factor that equals the standard deviation of a uniform distribution of width one.

It is important to note that the shear component in equation (3) is the product of the vertical dispersion, z, and the wind shear, du/dz. Wind shear alone cannot cause a large x. In fact, in actual boundary layers, z and du/dz tend to be negatively correlated(i.e., under convective conditions z will be large and du/dz will be small, whereas under stable conditions the reverse will be true).

The theoretical analyses by Chatwin[1] and Wilson[3] are based to some extent on a similarity theory, and both lead to a general agreement that x is approximately equal to a constant times u*t, where the constant is estimated to be somewhere between 1.0 and 3.0. There are several ways to derive this result, yet the simplest is to assume a ground-based puff in equation (3), for which the vertical dispersion, z, equals a constant, D, times the mass median height of the puff, zm(for Gaussian distributions, D is about 0.7). Then further assume that the atmosphere is neutral, for which du/dz at the height, zm, equals u*/(0.4zm). Consequently, xs = 0.5 u* t, which is the same functional form as the first (turbulent component) term in equation (2).

Despite the apparent simple result given for xs in the above derivations, it is important to note that the influence of the mean wind shear is difficult to parameterize in the boundary layer, since the wind shear is a strong(inverse) function of height. For example, du/dz is ten times as large at a height of 2 m as it is at a height of 20 m. The constant in equation (3) should be calibrated with data.

b. Van Uldens Formula for Ground-Level Releases

Van Uldens[2] formula for x, based on the continuity equation for the transport and diffusion of a passive cloud, requires the solution of a differential equation. Monin-Obukhov's similarity theory is employed to specify the eddy diffusivities and the wind speed profile, and the mean local turbulent mass fluxes are written according to the gradient transfer assumption, where the horizontal components of the turbulence are assumed to be homogeneous. The vertical eddy diffusivity Kz is taken to be equal to the eddy diffusivity for heat. $\sigma_s = \overline{(x - x_c)z}/\sigma_z \,.\, \bar{K}_x \,i\, \bar{K}_x = \alpha\sigma_d\sigma_u$, where is an empirical constant assumed to equal 0.3, and u is the standard deviation of the wind speed fluctuations in the along-wind direction. For the purposes of the current study, the model was solved numerically for four of the field experiments (Dugway Proving Ground, Nevada Test Site / Yucca Flat and Nevada Test Site / Frenchman Flat with ERP and URA configurations, see Section 3 for details of the experiments) and was found to yield results not much different from the proposed simple similarity formula. s the average horizontal relative eddy diffusivity, parameterized as The rate equation for the diffusing variance d is obtained by multiplying the diffusion equation by x2 and integrating over the whole space, assuming, based on van Ulden's[2] method, that the total along-wind or longitudinal variance of a cloud

x2 is obtained by the sum of the centroid variance(a deterministic component) and the diffusing variance(a random component). The centroid variance is defined as the horizontal along- wind variance of the local cloud centroid xc(z) calculated with respect to the cloud mass center. As such, it is a measure of the tilt of the cloud centerline with respect to a vertical line. The centroid variance can be conveniently approximated by the square of the skewness parameter, s, defined as

c. Assumptions Concerning Effective Puff Speed, ue.

The second variable of interest is the effective speed, ue, of the puff. Modelers have derived a simple method where ue can be assumed to equal the wind speed at a height of about 0.6 z for ground-based puffs. However, the exact value of the constant, 0.6, is still open to discussion. If observations of vertical profiles of the concentration and wind speed are available at a field site, ue can be calculated directly via a concentration-weighted integration of the puff with height.

In nearly all cases(except for the LROD experiment described in Section 3) the puff observations were made using fixed concentration monitors, which were oriented in nearly equally-spaced groups of monitors in the cross-wind direction at certain down-wind distances. Thus since x was not directly observed, the observed concentration time series(usually given as 1-second averages) were used first to estimate t. The effective speed, ue, can also be directly estimated from these observations based on knowledge of the time between the puff release and the arrival of the center of the puff at the monitor. However, in this case, ue is not a local value but represents an average over the total path of the cloud. Thus x can be calculated to equal uet. For some experiments(e.g., Dugway Proving Ground and Nevada Test Site / Yucca Flat experiments), the value of t was calculated by the usual second-moment method. For the Nevada Test Site / Frenchman Flat experiments and for most puff trials in the Hanford Kr-85 experiments, the concentration (C) time series were scanned in order to identify the time interval, dt0.1, between the times when the concentration first rose above 0.1 Cmax and last dropped below 0.1 Cmax, and t was calculated as dt0.1/4. Similarly, for some of the puff trials with missing or unreliable data at lower concentrations, the time interval dt0.5 between the two times corresponding to Cmax/2 was identified and t was calculated as 0.42dt0.5. For still other experiments t was calculated as 1/(4.3) times the duration of the time that the cloud was present over the monitors[10].

It should also be noted that the preferred basic data set should consist of cross-wind summed concentrations, in order to minimize the effect of internal puff variability and horizontal wind shears. However, if the puff trajectory is not perpendicular to the monitoring line, the concentration time-series recorded by each monitor on the line must to be corrected to account for the delay or off-set between the arrival times at the various monitors. For many of the older experiments the cross-wind data were no longer available and a concentration time series from single-monitors had to be used to calculate t.

d. Cloud Distortion at Large Distances

Many of the data sets analyzed in this paper involved puff dispersion over mesoscale or regional times and distances. As Gifford[11] and Smith[12] mention, contaminant clouds become very convoluted after a substantial time and distance due to the action of mesoscale and synoptic wind fields, which tend to break up the cloud into streaks and patches with open spaces in-between. This break-up of the cloud typically occurs at travel times of an hour or more. There is a continuous spectrum of horizontal turbulence that acts to maintain a near-linear increase of cloud width with time out to travel times of several days. It is remarkable that Heffters[13] 35-year old parameterization for puff lateral spread, y(in meters) = (0.5 m/s) t(in seconds), has proved to fit recent data quite well. This simple relation fits Giffords[14] compilation of y versus t data from nine field experiments almost as well as the prediction of his random-force theory. The data cover y ranges from about 30 m to 200 km and the travel time ranges from about 30 seconds to 4 days.

After a few hours of travel, there is little to distinguish between the lateral dispersion parameter, y, and the along-wind dispersion parameter, x. The cloud has been broken up by the wind field such that it is equally dispersed by

turbulence and shears in all horizontal directions. There is no longer an x and y direction; instead there is simply one radial r, where r is the horizontal direction from the mass center of the cloud or puff. Therefore, Gifford's[14] y data and Heffter's[13] y formula should be equivalent to the along-wind dispersion component, x, at mesoscale and regional distances. Furthermore, Gifford argues that the effects of wind shears are implicitly included in the observations in his random force theory and Heffter's formula at mesoscale and regional distances. As a result, Heffter's linear y formula can be written in the same form as equation (1) by assuming that the constant of 0.5 m/s is an average v over the cloud trajectory. Since u*/u is roughly equal to 1/20 and v is roughly equal

Table 1. Summary of along-wind dispersion experiments, including source release characteristics, surface roughness length (zo), number of puff trials, monitoring distances, wind speed ranges, and stability ranges

Experiment	Release elevation	zo(mm)	Number of puff trials	Monitoring distances(m)	Wind speed range(m/s)	Stability
DTRA Phase 1	Ground level point source	0.3	23 ensembles	200, 300, 400, 800,1200.(Flxed arc, varying release point)	2 to 7	Mostly unstable to slightly unstable
Dipole Pride 26 daytime tests	Ground level point source	32	10	~11000	3 to 5	Unstable
Diploe Pride 26 nighttime tests	Ground level point source	32	5	~11000	2 to 5	Stable
Kit Fox ERP	Ground level point source	200	6	225	2 to 3	Stable
Kit Fox URA	Ground level point source	20	9	225	3 to 4	Stable
Kit Fox SSR	Ground level point source	0.2	6	225	2 to 3	Mostly neutral to stable
Hanford Kr-85	Ground level point source	30	6	200, 800	1 to 8	Stable to unstable
Marchwood wind tunnel	Ground level point source	0.3	150 to 300	1, 3, 5, 7	1 to 4	Neutral
LROD	90 m line source	0.02 to 0.86	11	~2500 to ~10000	3 to 11	Near neutral
Victoria	90 m line source	40	17	43000-185000	3 to 15	n/a
Oceanside	61 to 152 m line sources. Gound level point sources	n/a	15	23000	1 to 5	n/a
Ft. Wayne	91 to 244 m line sources	n/a	70	1600-12000	5 to 16	n/a
EAPJ	Ground level point source	n/a	22	1500-7000	n/a	Unstable to stable
SRDES	Ground level point source	n/a	21	20-100	1 to 2	n/a

to 1.8u*, then Heffter's formula is consistent with friction velocities, u*, of approximately 0.25 m/s and wind speeds of approximately 5 m/s, which are typical of the experimental conditions.

3. Description of Field Experiments and Wind Tunnel Experiment

An attempt was made to acquire as many along-wind dispersion observations from as many sites as possible. Existing literature was surveyed and several candidate data sets were identified in addition to recent data sets available as part of ongoing research studies by the current authors. Other data sets were acquired for analysis based on information reported in journal articles. A summary of the characteristics of the field experiments and wind tunnel study is given in Table 1. Note that data was available from over 100 puff field trials, from which over 600 observations could be obtained. In most cases, the concentrations were observed by stationary monitors arrayed along crosswind-arcs.

The Dugway Proving Ground(DPG) DTRA Phase I puff trials were carried out in order to evaluate puff dispersion models, which predict the ensemble mean and variance of a large number (an ensemble) of releases during similar conditions[15]. Each of the 23 trials represents a mean of the concentration time series observed over about 20 puff releases. The puffs were released near ground-level and the underlying surface was a flat desert with some vegetation. The single monitoring arc was located a few hundred meters downwind of the source(in practice, the monitoring arc was fixed and the downwind distance from the source to the monitoring arc was varied by moving the source).

The Nevada Test Site / Yucca Flat puff trials are known by the name Dipole Pride 26, and are broken down into day and night conditions in the subsequent analysis(d. tests and n. tests)[15,16]. The monitoring arc(Line 2 on Fig. 1) with six fast-response sensors was located about 11000 m from the source, which is an order of magnitude farther downwind than the monitoring distances at the DPG DTRA Phase I site. The locations of the source, monitoring arcs, meteorological stations, and terrain elevations are shown in Fig. 1. This study was intended to provide data for testing puff models over mesoscale distances in complex terrain relative to time and space-varying wind fields. The source was near ground-level and the underlying surface was a desert with some brush.

The Nevada Test Site / Frenchman Flat experiments had the code name Kit Fox. Although the site was a flat desert, the investigators placed many rectangular plywood obstacles over a broad area in order to roughen the surface[17~19]. In one set of trials(the URA), the roughness elements were 20 cm tall, giving a roughness length of about 1 or 2 cm. In another set of trials (the ERP/URA), there were 2.4 m roughness elements placed in the area within 35 m of the source, giving a roughness length of about 10 or 20 cm. In a third set of trials (the Smooth Surface Roughness, or SSR) described by Coulombe et al.[20], the roughness elements were removed, leaving the smooth desert surface with a roughness length of about 0.02 cm. The data from the URA, ERP, and SSR experiments were analyzed separately. For all sets of Kit Fox experiments, dense CO2 gas was released from a 2.25 m^2 area source at ground level and the duration of the release was finite (~20 s). In order to minimize the effects of density and the finite duration releases as much as possible, the current study is restricted to the group of trials with a higher wind speed and to the most distant (225 m) monitoring arc.

The Hanford Kr-85 experiments involved near-ground releases of puffs of Krypton-85 tracer gas in a desert scrub environment on the grounds of the Battelle Pacific Northwest Lab[21,22]. Two monitoring arcs were located at 200 and 800 m downwind, respectively. Detailed meteorological observations were also made.

Draxler[10] summarized three U.S. Army along-wind dispersion studies from the 1960s. The Fort Wayne[23], Victoria[24], and Oceanside (Smith and Niemann, 1969) experiments all involved elevated instantaneous line source releases from jet airplanes and the elevations ranged from about 50 m to 200 m. Of course, the release was not truly instantaneous, since it took several minutes for the plane to traverse the release line. However, the release time was small compared to the travel time to the monitoring arcs, which were located several km downwind(about 2 to 12 km at Fort

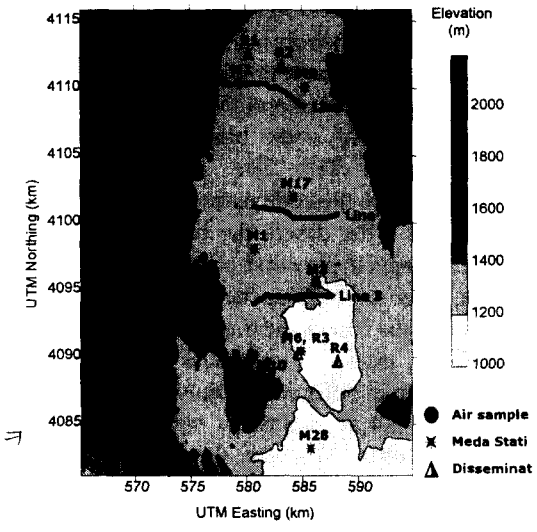

Fig. 1. Map of Dipole Pride 26 Field Site at Yucca Flat, Nevada Test Site[25]. Terrain contours are at 200 m separation, with dark shadings representing higher elevations. The releases took place at the disseminator locations marked as triangles. Meteorological observations were taken at Meda stations marked as stars. 15-minute average concentration observations were taken by air samplers, marked as circles, along three lines. The fast response concentration observations analyzed in this paper were taken by six samplers along Line 2.*

Wayne, 40 to 180 km at Victoria, and 23 km at Oceanside). The Fort Wayne releases were just upwind of a moderate-sized city and the Victoria and Oceanside releases were just offshore during onshore flows. Two different tracers, large 20 m particles (LP) and a yellow fluorescent pigment (YFP), were used at Victoria and are analyzed separately.

The Long-Range Overwater Dispersion(LROD) experiment was conducted within the overwater air space of the Pacific Missile Range Facility, Kauai, Hawaii[26]. It took place 30 years later than the three experiments described above but was similar in release type. The source was an instantaneous elevated(about 100 or 200 m) line source, released from an airplane. Although there were both surface monitors(boats) and airplane monitors, few of the boat data are useful because of high seas. The airplane flew racetrack patterns across the cloud, centered on a fixed longitudinal sampling line along which the boats were placed. The analysis treated the airplane and boat data separately.

Sato et al.[27] and Sato[28] reported on their Short Range Diffusion Experiment Series (SRDES), which involved near-ground releases of puffs in a field, with monitoring mostly at a downwind distance of about 20 m. Monitors were also placed on a tower, so that vertical concentration profiles could be obtained. Extensive turbulence data were observed by sonic anemometers, although only limited data are presented in the references. Sato et al.[27] also present data from the Environmental Assessment Program Japan (EAPJ) experiments, which involved the analysis of the leading and trailing edges of detached plumes, namely plumes generated by finite duration (30 min to 1 h) releases, and observed at downwind distances of a few kilometers.

The Marchwood wind tunnel data[29] focussed on ensembles of short duration releases of neutrally-buoyant gas released at ground-level under neutral boundary layer conditions that could be exactly replicated for each individual experiment of the ensemble. Very detailed concentration time series were obtained and analyzed from the point of view of a similarity theory.

With the exception of the LROD experiment, where x could be measured directly by the airplane flying back and forth across the cloud, all the other experiments involved the analysis of concentration time series observed by fixed monitors. For the fixed monitors, t is the parameter that is measured directly yet can be converted to x through the relation

$$x = uet \qquad (4)$$

where ue is the local effective advection speed of the cloud. In practice ue is usually estimated as x/tc, where x is the distance to the monitor and tc is the time after release when the center of the cloud passes the monitor.

4. Data Summary and Results

The data from the puff trials at the 13 field experiments and the wind tunnel experiment are

Table 2. Modelers data archive for all experiments analyzed. The data listed should be sufficient for reproducing the current results and for developing and testing alternate formulas for along-wind dispersion

	Test	Distance (m)	Release time (local time)	Travel time(sec)	u(m/s)	ue(m/s)	u*(m/s)	L(m)	σt(s)	σx(m)	σx/u*(s)
DARA Phase 1	T02	192	18:02	27.3	5.6	7.0	0.26	-36	2.9	20.6	79.2
	T01	192	17:15	27.8	5.9	6.9	0.26	-18	2.9	20.1	77.3
	T03	192	19:00	33.3	4.6	5.8	0.2	-79	3.4	19.5	97.7
	T09	356	19:34	82.2	4.6	4.3	0.19	-207	7.4	31.8	168
	T04	299	18:44	82.4	3.6	3.6	0.16	-20	6.2	22.6	141
	T08	356	18:10	85.8	4.4	4.2	0.19	-18	7.6	31.5	166
	T05	356	19:00	95.2	3.6	3.7	0.2	-4	6.3	23.7	119
	T07	356	16:48	110	3.2	3.2	0.15	-3	7.5	24.4	163
	T10	356	20:44	110	3.4	3.2	0.16	226	10.2	33.1	207
	T11	814	11:05	110	7.4	7.4	0.34	-72	8.4	62.4	184
	T12	814	14:01	120	6.9	6.8	0.3	-25	8.5	58.0	193
	T13	776	15:42	156	4.5	5.0	0.21	-11	11.3	56.4	269
	T16	356	14:20	157	2.0	2.3	0.08	-0.4	13.0	29.5	369
	T16	1203	14:21	167	7.1	7.2	0.32	-21	10.9	79.0	247
	T14	776	17:59	198	3.7	3.9	0.18	-34	16.5	64.3	357
	T17	1198	19:23	216	5.1	5.5	0.25	133	18.0	99.8	399
	T15	776	18:54	271	2.7	2.9	0.11	74	24.5	70.1	638
Dipole Pride 26	T162	11090	13:30	1634	5.1	6.8	0.36	-67	194	1319	3664
	T122	13151	10:30	1741	7.1	7.6	0.5	-71	152	1149	2299
	T171	10835	12:00	2331	4.9	4.7	0.34	-22	149	692	2034
	T141	11612	13:00	2232	4.6	5.2	0.34	-28	163	846	2487
	T161	10835	12:00	2570	4.8	4.2	0.34	-25	684	2889	8496
	T121	13177	9:00	2491	5.1	5.3	0.4	-72	181	956	2391
	T071	10835	13:00	2737	4.1	4.0	0.29	-24	151	596	2056
	T072	10835	14:45	2975	4.4	3.6	0.27	-41	94.8	345	1278
	T095	11612	14:00	3254	3.0	3.6	0.2	-46	131	467	2336
	T111	12329	14:30	4054	3.2	3.0	0.2	-30	300	911	4557
	T042	11294	5:38	2160	5.0	5.2	0.25	634	147	769	3074
	T041	11817	4:00	2483	4.9	4.8	0.23	26	173	822	3572
	T031	10747	4:00	2522	3.8	4.3	0.17	19	692	2948	17339
	T061	12329	4:00	4260	2.5	2.9	0.06	32	868	2508	41792
	T051	11460	4:40	4664	2.4	2.5	0.05	12	752	1849	36988
Kit Fox ERP	5_1	225	Sunset	72	3.0	4.5	0.42	167	11.6	52.2	124
	3_2	〃	〃	73	2.2	6.2	0.42	93	13.8	85.6	204
	3_3	〃	〃	91	2.0	4.0	0.4	74	16	64	160
	3_1	〃	〃	86	2.1	2.7	0.4	80	11.6	31.3	78.3
	5_2	〃	〃	89	2.3	4.6	0.42	99	13.8	63.5	151
	5_5	〃	〃	91	2.1	4.5	0.37	80	17	76.5	207
Kit Fox URA	8_2	225	Sunset	68	4.2	5.0	0.34	159	4	20	58.8
	6_2	〃	〃	77	3.7	4.2	0.34	150	8.2	34.4	101
	8_3	〃	〃	77	3.6	4.8	0.34	194	4	19.2	56.5
	6_1	〃	〃	74	4.2	6.2	0.32	194	8.2	50.8	159
	8_1	〃	〃	65	4.3	4.8	0.35	203	6.9	33.1	94.6
	8_7	〃	〃	91	3.0	3.7	0.27	80	10.5	38.9	144
	8_4	〃	〃	95	3.1	3.7	0.32	135	5.5	20.4	63.8
	8_6	〃	〃	75	3.4	3.9	0.27	93	14.9	58.1	215
	8_3	〃	〃	85	3.4	3.9	0.29	127	6.9	26.9	92.8

Table 2. Continued

	Test	Distance (m)	Release time (local time)	Travel time(sec)	u(m/s)	ue(m/s)	u*(m/s)	L(m)	σ t(s)	σ x(m)	σ x/u*(s)
Kit Fox SSR	T09R03A3	225	18:09	90	4	2.5	0.17	23	5.1	12.8	77.2
	T09R05A3	〃	18:20	103	3.3	2.2	0.13	12	6.6	14.3	108
	T09R06A3	〃	18:23	118	3.2	1.9	0.12	9.9	9.1	17.4	140
	T13R02A3	〃	18:15	122	2.8	1.8	0.11	7.9	5.7	10.5	96.5
	T13R04A3	〃	18:29	114	3.4	2	0.13	8.9	6.1	12.1	92.3
	T13R05A3	〃	18:30	107	3.7	2.1	0.15	1.0	7.4	15.6	106
Hanford Kr-85	T2arc1	200	23:00	391	1.3	0.5	0.05	Stab.Class:F	96	48	961
	T2arc2	800	23:00	779	1.3	1	0.10	Stab.Class:F	172	172	1724
	T3arc1	200	7:38	77.6	4.2	2.6	0.26	Stab.Class:D	12.4	32.2	124
	T3arc2	800	7:38	213	4.2	3.8	0.38	Stab.Class:D	30	114	300
	T5arc1	200	10:52	38.3	8	5.2	0.52	Stab.Class:C	7.5	39	74.9
	T5arc2	800	10:52	111	8	7.2	0.72	Stab.Class:C	13.8	99.4	138
	T6arc1	200	11:30	39.9	7.3	5	0.50	Stab.Class:C	7.8	39	78.3
	T6arc2	800	11:30	119	7.3	6.7	0.67	Stab.Class:C	13	87.1	117
	T7arc1	200	10:52	62.1	4.6	3.2	0.32	Stab.Class:C	20.8	66.6	208
	T7arc2	800	10:52	200	4.6	4	0.40	Stab.Class:C	19.7	78.8	197
	T8arc1	200	6:02	174	1.5	1.1	0.11	Stab.Class:E	37	40.7	370
	T8arc2	800	6:02	493	1.5	1.6	0.16	Stab.Class:E	92.5	148	925
LROD	Test 1	59776	9:05	7812	2.6	7.7	0.10	-76	169	1304	13583
	Test 2	4190-104116	7:10	755-10382	8.2	10.5	0.29	-1667	26-179	271-1877	948-6563
	Test 3	2478-108464	12:25	390-10859	9.8	10.1	0.34	-1250	16-256	164-2590	480-7573
	Test 6	9746-101894	6:02	813-8956	7.7	10.7	0.27	-400	25-148	267-1579	985-5827
	Test 7	6981-105766	10:48	460-8642	9.3	12	0.33	-909	24-165	286-1979	880-6089
	Test 8	9155-102674	15:26	802-8473	10.3	12.7	0.36	370	17-137	212-1734	597-4885
	Test 9	3485-123232	7:16	260-12645	10.3	10.1	0.36	-5000	17-347	167-3500	465-9749
	Test10	25669-113191	8:06	2345-11141	5.1	9.9	0.18	455	65-373	645-3690	3665-20966
	Test11	11386-98747	14:31	1104-9813	10.3	10.3	0.36	10000	25-246	259-2531	723-7070
	Test12	15205-47240	7:00	1182-3595	11.3	13.5	0.39	625	43-135	575-1816	1471-4645
	Test13	8933-100416	11:15	618-6551	11.3	15.6	0.39	476	16-304	245-4739	628-12151
Rt.Wayne	101data	1600-12000	n/a	720-10200	5-16	n/a	n/a	n/a	66-3060	n/a	n/a
Victoria	Test 1	48000-178000	19:30	7500-26100	5.8	5.9-6.8	0.20	n/a	840-4200	5376-28644	268800-143218
	Test 2	134000	19:31	24540	4.2	5.5	0.20	n/a	2520	13760	68802
	Test 3	48000-176000	19:30	7200-38700	5.2	3.2-8.6	0.10	n/a	2040-6000	13600-38306	13600-383059
	Test 4	43000-182000	19:30	4500-30300	5.6	4.1-12	0.20	n/a	1680-7740	13072-56768	65360-283838
	Test 5	43000-178000	19:30	7200-27000	4.2	3.9-8.4	0.20	n/a	420-4140	2100-34906	10500-174529
	Test 6	43000-174000	19:30	78000-32700	6.5	4-7.8	0.20	n/a	480-6000	1911-29762	9556-148810
	Test 7	48000-138000	19:15	8100-38700	4.2	2.9-5.9	0.30	n/a	420-7020	1223-23581	4077-78602
	Test 8	48000-138000	19:15	9000-35100	4.6	3.5-5.3	0.20	n/a	720-7020	3840-29092	19200-145459
	Test 9	43000-185000	19:15	4500-33300	6.6	4.1-12	0.20	n/a	1320-7980	6103-52589	30516-262943
	Test10	48000-134000	17:00	6600-29700	6.9	4.3-7.5	0.40	n/a	540-7200	3391-40000	8478-100000
	Test11	7600-94000	17:00	24300-31200	6	3-3.8	0.30	n/a	2820-5700	8496-19289	28321-64296
	Test12	48000-174000	17:00	11700-33300	5.8	2.9-5.2	0.60	n/a	900-7020	3692-20091	6154-33485
	Test13	43000-182000	17:00	3600-32100	6.3	4.3-15	0.50	n/a	480-6000	3235-36211	6470-72421
	Test14	48000-182000	17:00	6300-33300	7.6	5.1-8.6	0.50	n/a	720-4320	5486-29193	10971-58386
	Test15	85000-178000	17:00	16200-41400	4.8	4.3-6.3	0.40	n/a	1800-5760	9444-36814	23611-92035
	Test16	48000-128000	17:00	8000-29700	5.4	3.7-6.7	0.30	n/a	600-6600	3200-29110	10667-97032

Table 2. Continued

	Test	Distance (m)	Release time (local time)	Travel time(sec)	u(m/s)	ue(m/s)	u*(m/s)	L(m)	σ t(s)	σ x(m)	σ x/u*(s)
March-wood	Pos 1	0.83	Indoor exp.	2.1	1	0.51	0.047	Stab.Class:D	0.41	0.21	4.47
	Pos 2	2.5	Indoor exp.	5.5	1	0.6	0.047	Stab.Class:D	0.86	0.52	11.1
	Pos 3	4.17	Indoor exp.	8.4	1	0.64	0.047	Stab.Class:D	1.12	0.72	15.3
	Pos 4	5.93	Indoor exp.	11	1	0.69	0.047	Stab.Class:D	1.42	0.98	20.9
Oceanside	27	23000	17:57	12105	2.4	1.9	n/a	n/a	460	875	n/a
	28	23000	19:04	17692	2.2	1.3	n/a	n/a	614	798	n/a
	29	23000	19:06	20909	1.5	1.1	n/a	n/a	1451	1596	n/a
	30	23000	17:04	7667	3.4	3	n/a	n/a	237	712	n/a
	31	23000	15:05	6970	3.8	3.3	n/a	n/a	363	1197	n/a
	32y	23000	18:03	10952	2.5	2.1	n/a	n/a	753	1582	n/a
	32g	23000	18:03	10000	2.5	2.3	n/a	n/a	879	2022	n/a
	35y	23000	19:04	16429	2	1.4	n/a	n/a	544	762	n/a
	35g	23000	19:04	19167	2	1.2	n/a	n/a	558	670	n/a
	36y	23000	17:05	6970	2.9	3.3	n/a	n/a	209	691	n/a
	36g	23000	17:05	6970	2.9	3.3	n/a	n/a	195	645	n/a
	37y	23000	15:05	5349	5.4	4.3	n/a	n/a	251	1080	n/a
	37g	23000	15:05	4792	5.4	4.8	n/a	n/a	112	536	n/a
	38y	23000	17:05	6389	4.1	3.6	n/a	n/a	167	603	n/a
	38g	23000	17:05	6571	4.1	3.5	n/a	n/a	251	879	n/a
SRDES	18 data	20-100	n/a	6-120	1-2	n/a	n/a	n/a	1-15	n/a	n/a
EAPJ	M2	3400	12:30-13:30	1740	n/a	2.0	n/a	n/a	307	600	n/a
	T2	2500	15:00-15:28	2940	n/a	0.9	n/a	n/a	447	380	n/a
	T4	2500	11:00-11:30	810	n/a	3.1	n/a	n/a	321	991	n/a
	T5	2500	13:00-13:30	2550	n/a	1.0	n/a	n/a	209	205	n/a
	T5	5100	13:00-13:30	4350	n/a	1.2	n/a	n/a	363	425	n/a
	W1	1500	12:01-12:27	1440	n/a	1.0	n/a	n/a	307	320	n/a
	W1	5000	12:01-12:27	3960	n/a	1.3	n/a	n/a	642	810	n/a
	W2	1500	12:30-13:00	600	n/a	2.5	n/a	n/a	84	209	n/a
	W3	5000	12:30-13:00	1800	n/a	2.8	n/a	n/a	181	504	n/a
	W5	1500	12:30-13:00	960	n/a	1.6	n/a	n/a	265	414	n/a
	W6	1500	12:30-13:00	900	n/a	1.7	n/a	n/a	279	465	n/a
	S2	3000	14:11-14:30	840	n/a	3.6	n/a	n/a	265	947	n/a
	S2	7300	14:11-14:30	5040	n/a	1.4	n/a	n/a	209	303	n/a
	O1	2600	14:00-14:30	660	n/a	3.9	n/a	n/a	140	550	n/a
	O1	4700	14:00-14:30	2490	n/a	1.9	n/a	n/a	293	553	n/a
	O2	2600	14:00-14:30	660	n/a	3.9	n/a	n/a	140	550	n/a
	O2	4700	14:00-14:30	2790	n/a	1.7	n/a	n/a	433	729	n/a
	O3	4700	10:30-11:00	4230	n/a	1.1	n/a	n/a	181	202	n/a
	O6	2600	10:00-10:30	570	n/a	4.6	n/a	n/a	126	573	n/a
	N1	6950	16:07-16:30	3810	n/a	1.8	n/a	n/a	377	687	n/a
	N2	3450	10:00-10:30	2460	n/a	1.4	n/a	n/a	377	528	n/a
	N2	6950	10:00-10:30	3960	n/a	1.8	n/a	n/a	335	588	n/a
	N3	3450	10:40-11:10	1380	n/a	2.5	n/a	n/a	140	349	n/a
	N6	6950	15:30-16:00	4650	n/a	1.5	n/a	n/a	181	271	n/a

summarized in the Modelers Data Archive in Table 2, which contains the basic observations sufficient for a similarity analysis of the along-wind dispersion. This Modelers Data Archive should be useful to other researchers for developing and testing their own theories, although it may be necessary to refer to the data reports for additional data. It should be mentioned again that, with the exception of the airplane data from the LROD experiment, where x was directly observed, the basic observations consist of the puff t and travel time based on the observed concentration time series at each monitoring arc.

In order to test the similarity relations, it is interesting to present the combined data as plots of t versus t and x/u* versus t in a log-log format as in Fig. 2 and Fig. 3, respectively. About half of the points on the figures are a factor of two of the simple linear relations:

$$t = 0.1\ t \quad (5)$$

$$x/u^* = 1.8\ t \quad (6)$$

These formulas, which are drawn from the figures, provide a good fit with the data, which are from many different sites and which cover t over four orders of magnitude(from about 0.3 seconds to about 10,000 seconds) and travel times over four orders of magnitude(from about 2 seconds to about 30,000 seconds or 8 hours). The 1.8 u* t relation is in good agreement with the theoretical

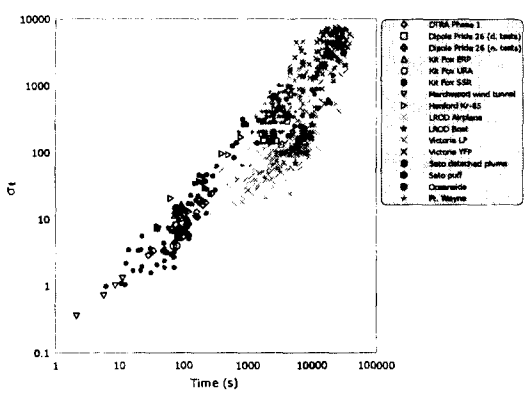

Fig. 2. Standard deviation of observed concentration time series, t, plotted versus observed travel time, t, for all experiments. The different symbols are explained in the legend. The line represents the formula t = 0.1 t.

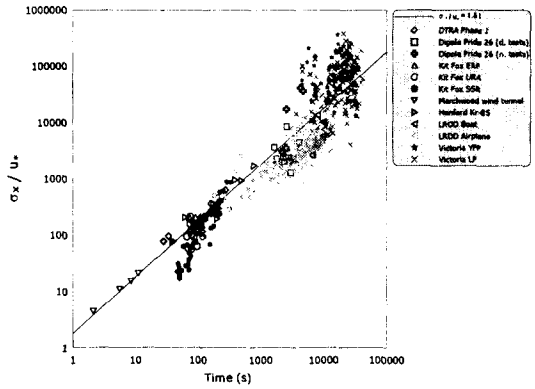

Fig. 3. Along-wind dispersion coefficient x = uet, divided by friction velocity, u*, and plotted versus observed travel time, t, for experiments listed in legend. The different symbols are explained in the legend. The line represents the formula x = 2 u* t.

prediction of equation (2) and prior analyses discussed in Section 2.

The accuracy of the x data in Fig. 3 depends on the accuracy of the assumed puff advective speeds, ue, which are used to calculate x = t ue. The observed puff effective speeds, ue, were found to be within 10 or 20 % of the observed wind speeds at the Nevada Test Site / Yucca Flat experiments. Hanna and Chang[17] found that, for ground level puff releases, modeled peak concentrations were sensitive to the assumed puff advective speed.

Figs. 2 and 3 show that certain groups of points, representing specific field trials, are displaced from the line of best agreement. In some cases, this displacement can be explained due to the sampling methodology. For example, some t observations were based on time series of cross-wind summed concentrations, whereas others were based on the concentration time series at a single point (intuition would suggest that the t from the cross-wind summed data would be larger than the t from the point data). In other cases, the displacement of points on the figure may be due to fundamental physical causes. Of course, in Fig. 3, there may be errors in the u* estimates. However, this same type of scatter from one field experiment to another is always seen in field data, as shown by the plot in Gifford's (1995) paper[14].

The disparity in the number of points from one

field experiment to the next hampers the visual inspection of Figs. 2 and 3. For example, there are dozens of points for the Victoria and LROD data yet only a few for Dipole Pride 26. Accordingly, it is better to train the eye to equally weight the experiments rather than be influenced by the total number of points.

Acknowledgement

This work was supported by the Korea Institute for Science & Technology Evaluation and Planning (2000-J-ND-01-B-11).

References

[1] Chatwin, P.C., 1968 : The dispersion of a puff of passive contaminant in the constant stress region. *Quart. J. Roy. Met. Soc.*, 94, 350~360.

[2] Van Ulden, A.P., 1992 : A surface-layer similarity model for the dispersion of a skewed passive puff near the ground. *Atmos. Environ.*, 26A, 681-692.

[3] Wilson, D.J., 1981 : Along-wind diffusion of source transients. *Atmos. Environ.*, 15, 489~495.

[4] Sykes, R.I. and D.S. Henn, 1995 : Representation of velocity gradient effects in a Gaussian puff model. *J. Appl. Meteorol.*, 34, 2715~2723.

[5] Taylor, G.I., 1953 : Dispersion of soluble matter in solvent flowing slowly through a tube. *Proc. Roy. Soc. A*, 219, 186~203.

[6] Pasquill, F., 1969 : The influence of the turning of wind with height on crosswind diffusion. II. Meteorological Aspects of Air Pollution. *Phil. Trans. Roy. Soc. London A*, 265, 173~181.

[7] Csanady, G.T., 1969 : Diffusion in an Ekman layer. *J. Atmos. Sci.*, 26, 414~426.

[8] Saffman, P.G., 1962 : The effect of wind-shear on horizontal spread from an instantaneous ground source. *Q. J. Roy. Met. Soc.*, 88, 382~393.

[9] Smith, F.B., 1965: The role of wind shear in horizontal diffusion of ambient particles. *Q. J. Roy. Meteorol. Soc.* 91, 318~329.

[10] Draxler, R.R., 1979 : Some observations of the along-wind dispersion parameter. 4th Conf. on Turb. and Diff., AMS, 45 Beacon St., Boston, 5~8.

[11] Gifford, F.A., 1989 : The shape of large tropospheric clouds, or very like a whale. *Bull. Am. Meteorol. Soc.*, 70, 468~475.

[12] Smith, F.B., 1998 : Estimating the statistics of risk from a hazardous source at long range. *Atmos. Environ.*, 32, 2775~2791.

[13] Heffter, J.J., 1965 : The variation of horizontal diffusion patterns with time for travel periods of one hour or longer. *J. Appl. Meteorol.*, 4, 153~160.

[14] Gifford, F.A., 1995 : Some recent long-range diffusion observations. *J. Appl. Meteorol.*, 34, 1727~1730.

[15] Biltoft, C., 1997 : Phase I of DSWA transport and dispersion model validation study. DPG-FR-97-058. Dugway Proving Ground, UT 84022-5000.

[16] Watson, T.B, R.E. Keislar, B. Reese, D.H. George and C.A. Biltoft, 1998 : The DSWA Dipole Pride 26 Field Experiment. NOAA Tech Memo ERL ARL-225, ARL, Silver Spring, MD, 90 pages.

[17] Hanna, S.R. and J.C. Chang, 1999 : Testing of the HEGADAS model using the Kit Fox field data. Proceedings, Int. Conf. and Workshop on Modeling the Consequences of Accidental Releases of Hazardous Materials. AIChE, 3 Park Ave., New York, NY 10016~5901.

[18] Hanna, S.R. and K.W. Steinberg, 1996 : Studies of dense gas dispersion from short-duration transient releases over rough surfaces during stable conditions. *Air Poll. Modeling and Its Applic. XI*, Plenum Press, New York, 481~490.

[19] Western Research Institute, 1998 : Final Report on the 1995 Kit Fox Project, Vol. 1 Experimental Description and Data Processing, and Vol. 2 Data Analysis for Enhanced Roughness Tests. WRI, Laramie, WY, 109 + 67 pages.

[20] Coulombe, W., J. Bowen, R. Egami, D. Freeman, D. Sheesley, J. Nordin, T. Routh, and B. King, 1998 : Characterization of Carbon Dioxide Releases Experiment 2. Report No. 97-7240.1D, Desert Research

Institute, Reno, NV.

[21] Nickola, P.W., J.D. Ludwick and J.V. Ramsdell, Jr., 1970 : An inert gas tracer system for monitoring the real-time history of a diffusing plume or puff. *J. Applied Meteorol.*, 9, 621~626.

[22] Nickola, P.W., J.V. Ramsdell, Jr. and J.D. Ludwick, 1970: Detailed Time-Histories of Concentrations Resulting from Puff and Short-period Releases of an Inert Radioactive Gas : A Volume of Atmospheric Diffusion Data, BNWL-1272, UC-53, Battelle Memorial Institute, Pacific Northwest Laboratories, Richland, WA 99352.

[23] Smith, T.B. and R.L. Miller, 1966 : Victoria Diffusion Trials, Vol. I. MRI-66-FR-374, Meteorological Research Inc., Altadena, CA 91001, 181.

[24] Smith, T.B. and B.L. Niemann, 1969 : Shoreline Diffusion Program, Oceanside, CA, Vols. I, MRI-64-FR-860, Meteorological Research Inc., Altadena, CA 91001.

[25] Biltoft, C., 1998 : Dipole Pride 26: Phase II of DSWA transport and dispersion model validation study. DPG-FR-98-001. Dugway Proving Ground, UT 84022-5000.

[26] Bowers, J.F., G.E. Start, R.G. Carter, T.B. Watson, K.L. Clawson and T.L. Crawford, 1994 : Experimental Design and Results for the Long-Range Overwater Diffusion(LROD) Experiment, DPG/JCP-94/012, U.S. Army Dugway Proving Ground, Dugway, UT 84022-5000.

[27] Sato, J., 1995 : An Analytical Study on Longitudinal Diffusion in the Atmospheric Boundary Layer. *The Geophysical Magazine, Series 2*, Vol. 1, No. 2, Japan Meteorological Agency, Tokyo.

[28] Sato, J., F. Kimura and T. Yoshikawa, 1981 : The longitudinal spread of puff in the short range diffusion experiment. *Papers in Meteorol. and Geophys.*, 32, 155~162.

[29] Robins, A.G. and J.E. Fackrell, 1998 : An experimental study of the dispersion of short-duration emissions in a turbulent boundary layer. *Air Pollution VI*(C.A. Brebbia, C.F. Ratto and H Powers, eds.), WIT Press, Southampton, 697~707.